

Accurate electronic excitations for two alkali-halide systems obtained by density-functional theory and verified by multi-configuration self-consistent field calculations

A. Hellman²³ and M. Slabanja

Department of Applied Physics, Chalmers University of Technology and Göteborg University, SE-412 96 Göteborg, Sweden.

Abstract

Use of density-functional theory in a Δ self-consistent field framework result in both the ground- and two lowest electronically excited states of the NaCl and LiCl. The accuracy of this method is confirmed using a multi-configuration self-consistent field method to obtain the same states. The overall good agreement between the calculated ground and excited potential-energy surfaces speaks promising for the computationally simple Δ self-consistent field method.

Keywords: multi-configuration self-consistent field calculations, density-functional calculations, Δ self-consistent field, electronic excitation

I. INTRODUCTION

The development of powerful computers has allowed available *ab initio* methods to calculate electronic excitations within considerably larger systems than ever before¹. However, the need to calculate electronically excited states within systems of such a size, that the above methods are just not practical, is ever present.

The less computational expansive density-functional theory² (DFT) as proved its value as a theoretical method over the years. Typically this method address only ground-state properties. However, over the years there has been a number of studies extending DFT into the realm of electronic excitations. Time-dependent DFT³, GW⁴, perturbation-DFT⁵ and embedded DFT⁶ methods, all show an impressive and promising progress in this field.

In this paper, DFT within a Δ self-consistent field (SCF) framework is used to calculate the ground and two lowest electronically excited states of NaCl and LiCl. The DFT-based Δ SCF method, which recently has received some justification⁷ is an extraordinary simple method to calculate electronic excited states. Here, state-of-the-art multi-configuration self-consistent field (MCSCF) method⁸ is used to confirm the accuracy of the above method by calculating the same electronic excitations. The calculated PES's obtained by both methods are compared both with other theoretical results⁹ and experimental¹⁰ ones. The overall agreement between the MCSCF method and the DFT-based Δ SCF method is promising for use of the Δ SCF method on systems of such size that are beyond the present realm of the MCSCF method.¹¹

As an extantion, the quantum dynamics of a simulated photodissociation process is resolved using time-dependent wavepacket propagation, on the obtained PES's. The wavepacket is simultaneously propagated on the coupled diabatic PES's and the distribution of the amplitudes are monitored at each timestep so that the dissociation fraction can be determined and also the intermediate dynamics of the photoreaction.

The organization of the paper is as follows. In section II the model and the computational methods used in this paper are described. Results from the calculation are presented in section III. Conclusions are given in section IV. Finally, the appendix state the results of a simulated photodissociation of the two alkali-halide systems

II. THEORY AND COMPUTATIONAL METHOD

The main advantage with an *ab initio* calculation, such as the MCSCF method, is the predictive power in estimating the fundamental forces that act on the involved nuclei, both in the ground state and in an excited state. Unfortunately, the highly accurate *ab initio* method is hard to apply to larger systems, due to the high computational cost. On the other hand, first-principle DFT has proven to be an essential tool in describing large systems, whereas it has been restricted to ground-state properties so far. However, recently ordinary DFT has been extended to include electronically excited states in a Δ SCF-fashion,⁷ with a working accuracy.¹¹

The optimized geometry was obtained by a restricted Hartree-Fock (RHF) calculation using GAMESS.¹² Here the basis set uses Slater-type orbitals (STO) together with 6 Gaussians, hence STO-6G. Both dimers have a C_{2v} point group symmetry, in which the Hamiltonian matrix is constructed in a basis that transforms according to the $A_1(\Sigma^+, \Delta)$, $B_1(\Pi)$, and $A_2(\Sigma^-, \Delta)$ irreducible representations. Here only the Σ^+ symmetry is considered since one of the aims is to simulate a photodissociation event. In addition, the use of symmetry reduces the complexity of the calculation substantially. The wavefunction obtained from the RHF calculation is used as an input to the MCSCF calculation, where 10 electrons are distributed in 14 active orbitals. This generate approximately one million sets of configuration determinants for the A_1 symmetry group. The MCSCF determines the PES's for the ground $^1\Sigma^+$ and the excited $^3\Sigma^+$, $^1\Sigma^+$ states with high accuracy.

In analogy with the Δ SCF¹³ method to calculate electronically excited states within the Hartree-Fock (HF) approximation, the DFT-based Δ SCF method uses different electronic configuration in the Kohn-Sham (KS) model system to represent these electronically excited states. Such an application of the KS formalism has for long been without any formal justification, but in a recent article by A. Görling⁷ this method retrieves some justification and indeed can be viewed as an approxima-

tive method to calculate electronic excitations within the considered system.

The methodology of the used DFT-based Δ SCF method is presented in length elsewhere¹¹ and here only a short description is given. The basic ingredients are three concepts: (i) interpretation of the KS-orbitals in a molecular orbital (MO) scheme, (ii) discretization of these orbitals and their energy levels, using supercell calculations with periodic boundary conditions, and (iii) introduction of electron-hole (e-h) pairs in the system, which is equivalent to an internal charge transfer in the supercell. First an ordinary DFT calculation is performed to obtain the ground state PES of the system and the KS orbitals with discrete energy levels. Then the relevant KS orbitals for the desired internal charge transfer process are identified as the ones that should be occupied in the ground state but unoccupied in the excited electronic configuration. Next a hole is introduced in one of these identified occupied KS orbitals together with an extra electron onto another one that is introduced into the excited configuration. In this way a KS determinant for the desired excitation is constructed. Finally, this KS determinant is optimized in a self-consistent-field calculation, and its energy is evaluated as in a normal DFT calculation. The total energy difference between the excited- and ground-state electronic configurations is identified as the excitation energy.

This method is straightforward, when calculating the covalent triplet $^3\Sigma$ state of the NaCl and LiCl dimers, since it can be constructed using only one KS determinant. However, in the photodissociation process the transitions from the ionic ground-state $^1\Sigma$ to the excited state $^3\Sigma$ is forbidden. Therefore we apply the so called “sum-method”¹⁴ to calculate the singlet $^1\Sigma$ state of the NaCl and LiCl dimers. Simply, it means that a weighted sum of determinants is constructed, including both the $^3\Sigma$ and $^1\Sigma$ state, and its energy is found by means of ordinary minimization procedure. After that, the energy for the singlet state can be extracted since the sole energy for the triplet state can be found by similar means.

The first principle calculations presented in this paper are performed by means of the plane wave pseudopotential code DACAPO¹⁵. The generalized-gradient (GGA) approximation^{16,17,18} is used for the exchange-correlation energy-density functional. The wave functions are expanded in a plane-wave basis set, and the electron-ion interactions are described by ultrasoft pseudopotentials. The electronic density between iterations is updated by means of a Pulay-mixing algorithm. The occupation numbers are updated using a developed technique based on minimization of the free energy functional. All calculations are performed allowing for spin polarization. The dimer cases LiCl and NaCl, are calculated using a supercell of a volume of $20 \times 20 \times 20 \text{ \AA}^3$. The reason for using such a big supercell is to minimize any artificial effect from the periodicity.

III. RESULT AND DISCUSSION

Here the results for total energies and aspects of the electronic structure, such as the charge density, are presented. The electronic ground states for the NaCl and

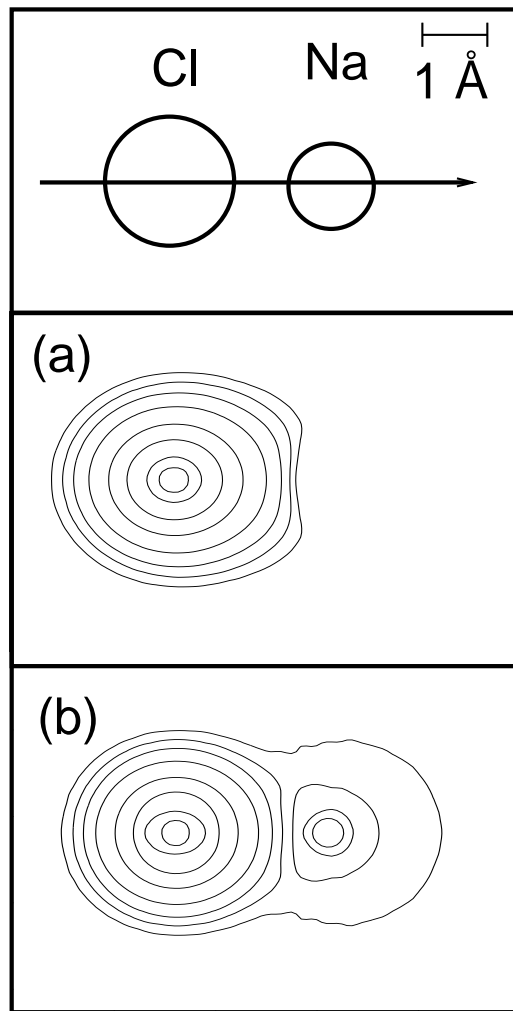


FIG. 1: The different valence electron density profiles of the NaCl molecule through a cut along the molecular axis. (a) The ground state with its ionic character, (b) The covalent $^3\Sigma$ state between Na and Cl.

LiCl dimers at their equilibrium distances are ionic, with the Na(Li) and Cl atoms being positively and negatively charged, respectively. However, at infinite separation the ground state is a neutral “covalent” configuration, where the ionic configuration lies about 1.4(1.7) eV above the covalent PES. This value comes from the difference in the ionization energy for the Na(Li) atom and the affinity energy of the Cl atom. As the Na(Li) and Cl atom move toward each other, there occurs at some intermediate separation ($\sim 10 \text{ \AA}$)⁹ approximate the PES’s for the covalent and ionic states have comparable energies, which makes an internal charge transfer of the unpaired 3(2)s electron on the Na(Li) to the electronegative Cl atom

and the electrostatic force affect the ionic fragment more strongly than in the original weak covalent bond. The ionic character of the ground state can be seen in Fig. 1a where the cut through the dimer axis clearly shows how the charge is focused around the chloride atom.

Analyzing the DOS for the system shows that the electron transfer moves the $3s$ -electron from the sodium atom to the empty $3p^6$ orbital on the chloride atom, as expected. So in order to obtain the excited triplet $^3\Sigma$ covalent state, the hole is introduced in the now filled $3p^6$ orbital and the electron in the parallel spin-channel of the $3s$ orbital of the Na atom. Figure 1b shows the covalent character of the excited $^3\Sigma$ state with a charge density located around the sodium atom, representing the $3s$ electron, and more importantly, a concentration of charge between the atoms. Since we are interested in the excited singlet $^1\Sigma$ state, we construct a combination of the triplet state and the singlet state by calculating the energy for the KS-determinant constructed by instead placing the electron in the anti-parallel spin-channel of the $3s$ orbital of the Na atom. The energy separation of the triplet-singlet state is then extracted from this calculation.

In Fig. 2 the PES's for the ionic $^1\Sigma$ ground state and both covalent $^3\Sigma, ^1\Sigma$ excited states of the NaCl dimer are shown, calculated with the MCSCF method and DFT-based Δ SCF method. In Table 1 the bondlength,

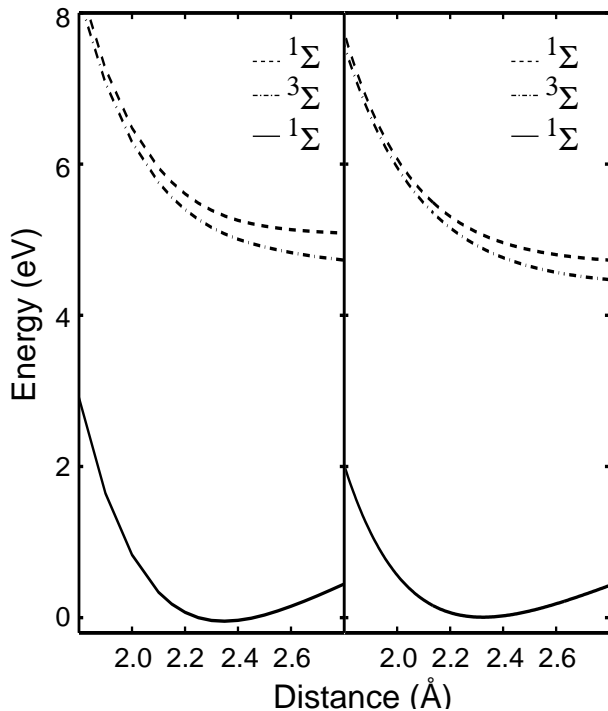


FIG. 2: The calculated potential energy curves for the NaCl system with the MCSCF (left) and Δ SCF methods (right). The ionic $^1\Sigma$ ground state is displayed in a solid line while the excited $^3\Sigma, ^1\Sigma$ covalent states use a dashed line.

and vertical excitation energies calculated with the

TABLE I: The calculated bondlength for the ionic $^1\Sigma$ state and vertical excitation energies to both $^3\Sigma, ^1\Sigma$ states, for the NaCl and LiCl dimers. Here results from (a) the MCSCF method, (b) the Δ SCF method, are compared with those for (c) the valence-bond (VB) method, and experiment. The unit is eV.

NaCl	MCSCF	Δ SCF	VB	Exp.
Bondlength	2.35	2.32	2.34	2.36
$^1\Sigma \rightarrow ^3\Sigma$	5.27	4.92	-	-
$^1\Sigma \rightarrow ^1\Sigma$	5.49	5.17	5.74	5.26
<hr/>				
LiCl				
Bondlength	2.02	2.06	2.07	2.02
$^1\Sigma \rightarrow ^3\Sigma$	5.96	5.64	-	-
$^1\Sigma \rightarrow ^1\Sigma$	6.08	5.75	7.28	-

present methods are compared with values from other calculations⁹ and experiment,¹⁰ for both the NaCl and LiCl dimers. The overall agreement between the point from the MCSCF and Δ SCF methods is promising. For instance, the discrepancy in the (i) vertical excitation for a $^1\Sigma \rightarrow ^1\Sigma$ transition for both the NaCl and LiCl dimers is around 0.3 eV, (ii) singlet-triplet splitting is around 0.05 eV, and (iii) bondlength is around 0.03 Å.

IV. CONCLUSIONS

The ground and two lowest excited states of NaCl and LiCl dimers are calculated. In the paper there are two main theoretical methods used; (i) the ab initio MCSCF method with high accuracy and (ii) a first-principle DFT-based Δ SCF method with a working accuracy to calculate both the ionic $^1\Sigma$ ground state and the two $^3\Sigma, ^1\Sigma$ covalent states of the systems.

The overall agreement between results of the MCSCF and DFT-based Δ SCF methods is very promising. For instance, the discrepancy in vertical excitation for a $^1\Sigma \rightarrow ^1\Sigma$ transition for both the NaCl and LiCl dimer is around 5% and in bondlength around 2% compared to each other.

V. ACKNOWLEDGMENTS

The work is supported by the Swedish Scientific Council and the Swedish Foundation for Strategic Research (SSF) via Materials Consortia No. 9 and ATOM-ICS, which is gratefully acknowledged. We thank B. I. Lundqvist for comments on the manuscript.

VI. APPENDIX

Knowing the PES's for the system enables the use of wavepacket propagation to resolve the quantum dynamics of the nuclei. However, the quantum dynamics of the photodissociation process on its multitude of diabatic potentials is a complex problem. As the system makes a sudden transition from its ground state to its excited state there will be a new set of forces that work on the dimer. The potential energy will be released into the intermolecular coordinate which might result in a dissociation of its fragments. The timeevolution of the system is determined by the Schrödinger equation

$$i\hbar \frac{\partial \Psi}{\partial t} = \hat{H} \Psi, \quad (6.1)$$

where the Hamiltonian matrix for the NaCl dimer looks like

$$\hat{H} = \begin{bmatrix} \hat{H}_{cov} & \hat{V}_{12} \\ \hat{V}_{21} & \hat{H}_{ion} \end{bmatrix} \quad (6.2)$$

Here the diagonal elements \hat{H}_{cov} and \hat{H}_{ion} represent well-defined electronic configurations of the NaCl and LiCl dimers, i.e. the ionic ground state and the covalent excited state. The off-diagonal element \hat{V}_{21} is the non-adiabatic coupling between the diabatic states, which enables the wavepacket to bifurcate among the states. It has been found¹⁹ that the strength of the non-adiabatic coupling term \hat{V}_{21} depends exponentially on the position of the curve-crossing point R_{cross} as

$$\hat{V}_{21} = V_{12} \exp[\gamma R_{cross}], \quad (6.3)$$

where for the halide Cl atom the parameters are $V_{12} = 20$ eV, $\gamma = 1.1638 \text{ \AA}^{-1}$.

The solution to the Schrödinger equation is calculated with a timedependent wavepacket method that is based on discrete variables and a finite basis representation (DVR-FBR).²⁰ The DVR has the advantage that the amplitude of the wavepacket is well defined, and it leads itself to the simultaneous propagation of the wavepacket on different diabatic potentials. The propagation of the wavepacket is done with the standard split operator technique²¹ where the potential operator together with the effect of the non-adiabatic coupling are evaluated in the DVR, while the kinetic operator is calculated in the FBR.

As a consequence of the overall good agreement between the PES's obtained by the MCSCF and DFT-based Δ SCF methods, the results from the quantum dynamics turns out to be the same within the simulations accuracy. Here the quantum dynamics performed by the NaCl dimer during photodissociation is found to be highly non-adiabatic, with a negligible population of the quasi-bound state, whereas the LiCl dimer has a small population of the quasi-bound state. It is concluded that the population of the quasi-bound state strongly depends

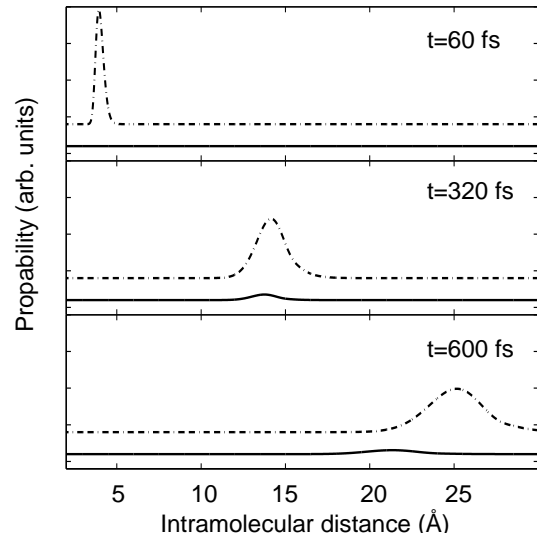


FIG. 3: The timeevolution of $|\langle \Psi(t) | \Psi(t) \rangle|^2$, representing the probability distribution for the NaCl dimer, at three different times. Here the dashed-dotted curve shows the probability distribution on the covalent state, whereas the solid curve is the probability distribution of the ionic state.

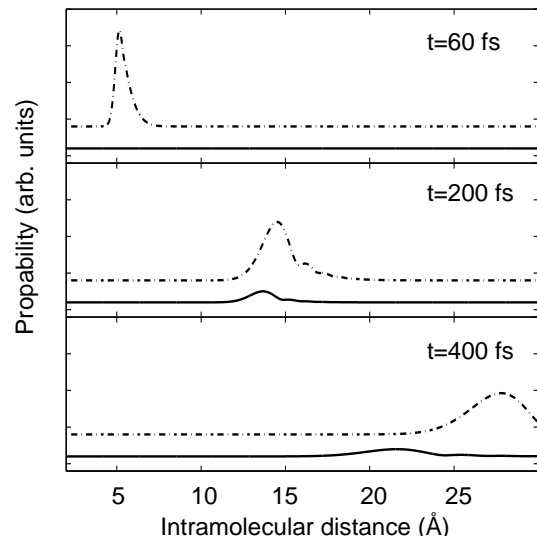


FIG. 4: The timeevolution of $|\langle \Psi(t) | \Psi(t) \rangle|^2$, representing the probability distribution for the LiCl dimer, at three different times. Here the dashed-dotted curve shows the probability distribution on the covalent state, whereas the solid curve is the probability distribution of the ionic state.

on the difference between the ionization potential and the affinity for the two atoms involved in the dimer. Hence, if one moves up the rows of the alkali-atoms or down the rows of the halogen-atoms the population of the quasi-bound state is expected to increase substantially. The observation of oscillations in pump-probe experiments on NaI dimers²² should be consistent with this conclusion.

-
- ¹ J. Pople, Quantum Chemical Models, Noble lecture, *www.nobel.se*, (1998).
- ² P. Hohenberg and W. Kohn, Phys. Rev. **136** (1964) B864; W. Kohn, and L. J. Sham, Phys. Rev. **140** (1965) A1133.
- ³ E. Runge and E. K. U. Gross, Phys. Rev. Lett. **52**, 997 (1984).
- ⁴ L. Hedin, Phys. Rev. **139**, A796 (1965).
- ⁵ A. Görling and M. Levy, Phys. Rev. B **47**, 13105 (1993).
- ⁶ T. Klüner, N. Govind, Y. A. Wang, and E. A. Carter, J. Chem. Phys. **116** (2002) 42.
- ⁷ A. Görling, Phys. Rev. A **59** (1999) 3359.
- ⁸ R. Shepard, in *Ab Initio Methods in Quantum Chemistry, Part II*, edited by K. P. Lawley John Wiley & Sons, New York 1987.
- ⁹ Y. Zeiri and G. G. Balint-Kurti J. Mol. Spectrosc. **99** (1983) 1.
- ¹⁰ J. A. Silver, D. R. Worsnop, A. Freedman, and C. E. Kolb, J. Chem. Phys. **84** (1986) 4378.
- ¹¹ A. Hellman, B. Razaznejad, and B. I. Lundqvist, J. Chem. Phys. **120** (2004) 4593.
- ¹² M. W. Schmidt, K. K. Baldrige, J. A. Boatz, *et al.*, J. Comput. Chem. **14** (1993) 1347.
- ¹³ J. C. Slater, Phys. Rev. **32** (1928) 339.
- ¹⁴ T. Ziegler, A. Rauk, and E. J. Baerends, Theor. Chim. Acta **43** (1977) 877.
- ¹⁵ B. Hammer, “computer code DACAPO-1.30”, Denmark Technical University, Lyngby, Denmark (1999).
- ¹⁶ J. P. Perdew *et al.*, Phys. rev. B **46** (1992) 6671.
- ¹⁷ J. P. Perdew, edited by P. Ziesche and H. Eschrig (Akademie Verlag, Berlin, 1991), Vol. 11.
- ¹⁸ J. P. Perdew, K. Burke and M. Ernzerhof, Phys. Rev. Lett. **77** (1996) 3865.
- ¹⁹ R. Grice, and D. R. Herschbach, Mol. Phys. **27** (1974) 159.
- ²⁰ R. Kosloff, in *Time-Dependent Quantum Molecular Dynamics*, edited by J. Broeckhove and L. Lathouwers Plenum Press, New York 1992.
- ²¹ M. D. Feit, J. A. Fleck, and A. Steigler, J. Comp. Phys. **47** (1982) 412.
- ²² T. S. Rose, M. J. Rosker, and A. H. Zewail, J. Chem. Phys. **91** (1989) 7415.
- ²³ Corresponding author: Tel. +46 31 772 3377; Fax: +46 31 772 8426; E-mail: ahell@fy.chalmers.se